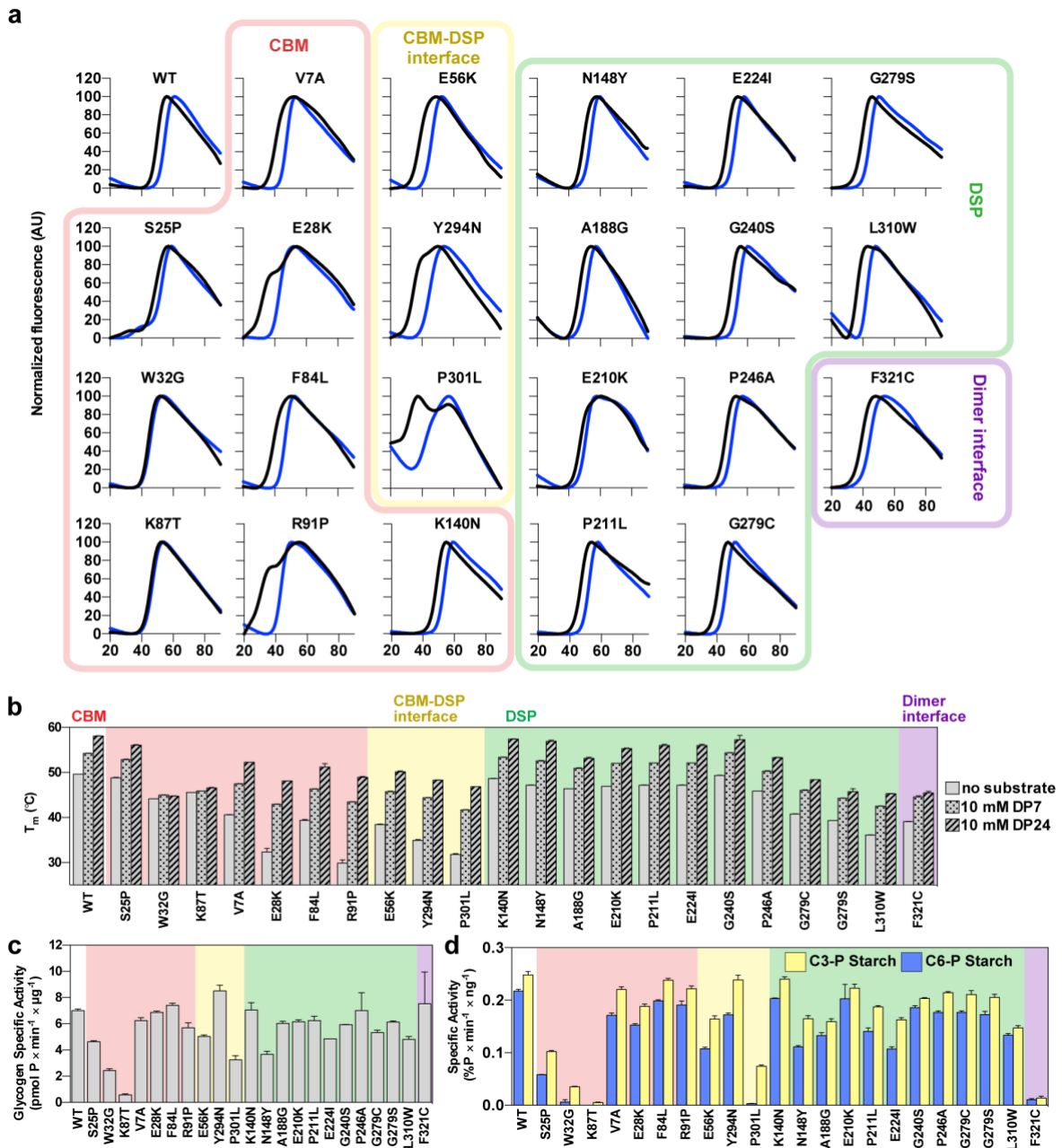


**Supplemental information**

**An empirical pipeline for personalized  
diagnosis of Lafora disease mutations**

**M. Kathryn Brewer, Maria Machio-Castello, Rosa Viana, Jeremiah L. Wayne, Andrea Kuchtová, Zoe R. Simmons, Sarah Sternbach, Sheng Li, Maria Adelaida García-Gimeno, Jose M. Serratosa, Pascual Sanz, Craig W. Vander Kooi, and Matthew S. Gentry**

## Supplemental Figures



**Figure S1. Stability, carbohydrate binding, and specific phosphatase activity of WT and mutant laforin, related to Figure 2.** (a) Melting profiles of WT laforin and mutants in the absence of substrate are shown in black. Melting profiles in the presence of 10 mM DP7 are shown in blue. Data are representative of 3 replicates. (b) Absolute  $T_m$  for WT and mutants without substrate and in the presence of 10 mM DP7 or 10 mM DP24. For mutants with biphasic melting, only the  $T_m$  corresponding to the first transition is shown. (c) Specific activity toward glycogen of WT and mutant laforin. (d) Specific activity toward C3-P and C6-P starch substrates of WT and mutant laforin. In (b) through (d) bar graphs represent the average of triplicate reactions  $\pm$  SD.

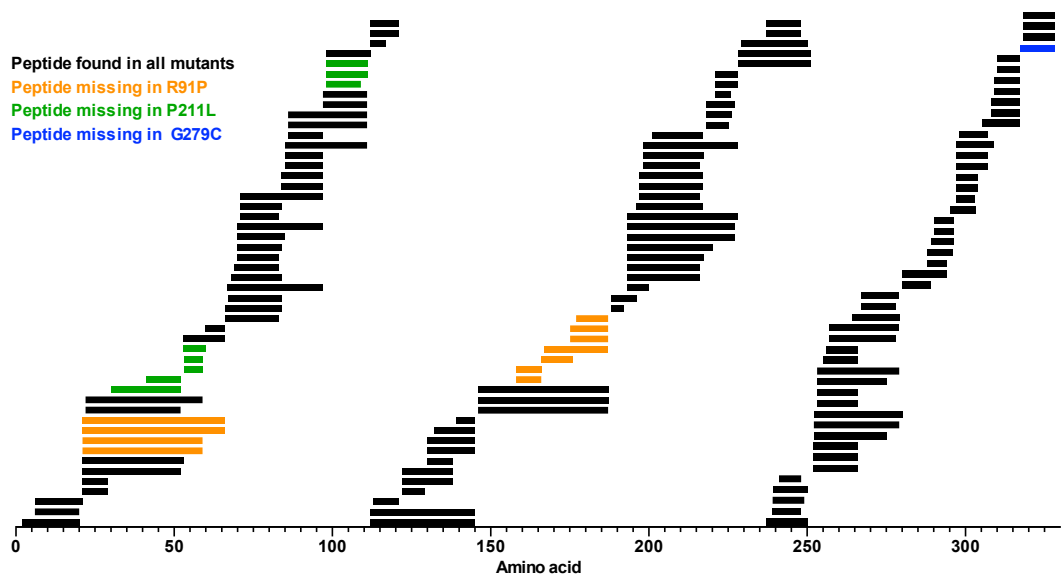


**Figure S2. HDX peptide coverage of selected laforin mutants, related to Figure 4.** Sequence coverage of WT laforin by pepsin-digested peptides. In all 4 mutants, 100% of residues 2 – 228 were covered by at least one peptide. A total of 148 high-quality peptides were identified. Digestion patterns of mutants were almost identical to WT with the following exceptions: R91P lacked 11 peptides (orange), P211L lacked 8 peptides (green), and G279C lacked 1 peptide (blue). F321C contained all peptides.

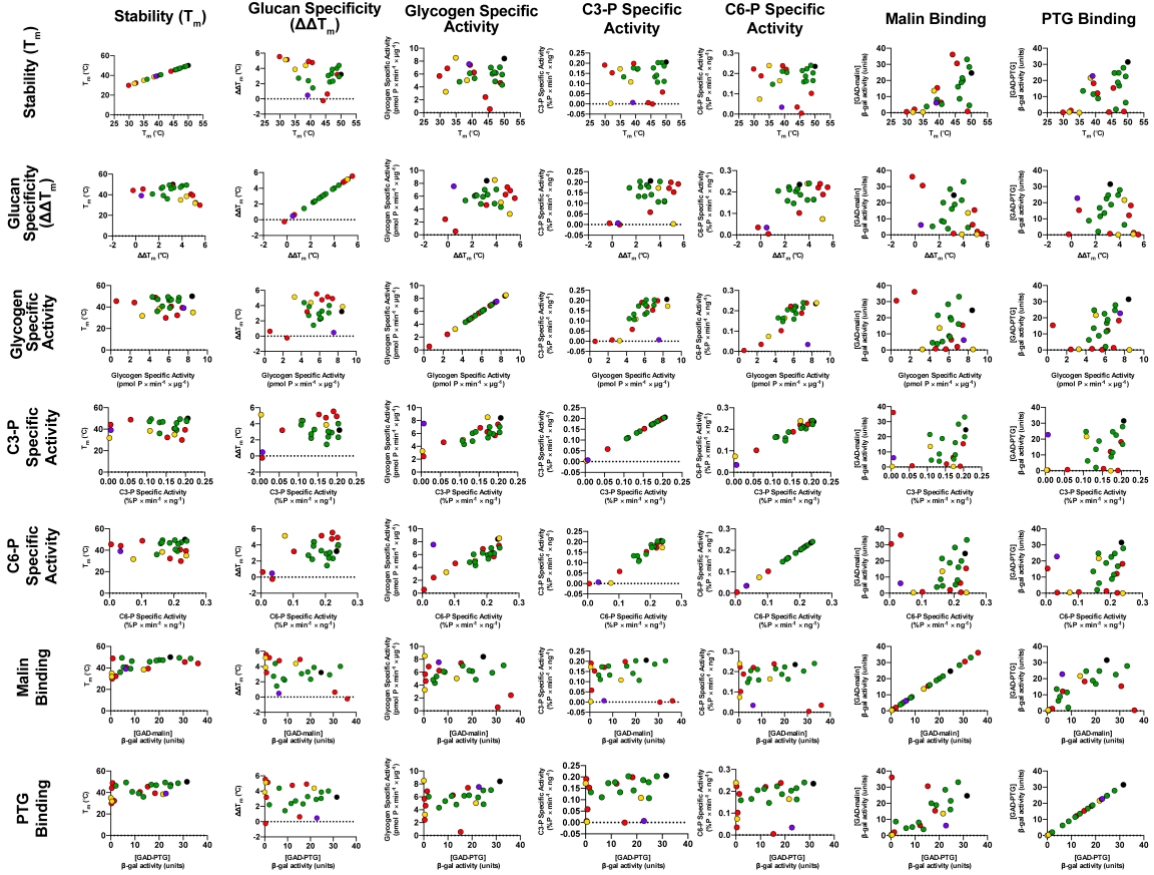


**Figure S3. Pairwise correlation plots of all laforin biochemical and functional measurements, related to Figure 5 and Table S1.** Nonparametric spearman correlations were used to compare laforin properties. Correlation coefficient ( $r$ ) and p-values are in Table S1. Datapoints are color coded by structural group: WT (black); CBM (red); CBM-DSP domain interface (yellow); DSP domain (green); dimer interface (purple).

		Stability (T <sub>m</sub> )	Glucan specificity ( $\Delta\Delta T_m$ )	Glycogen specific activity	C3-P specific activity	C6-P specific activity	Malin binding ( $\beta$ -gal activity)	PTG binding ( $\beta$ -gal activity)
<b>Stability (T<sub>m</sub>)</b>	Spearman r	1	-0.2955	-0.005929	0.2141	0.09289	0.6087	0.499
	P (two-tailed)		0.1711	0.9786	0.3266	0.6734	0.0021	0.0154
	P value summary		ns	ns	ns	ns	**	*
<b>Glucan specificity (<math>\Delta\Delta T_m</math>)</b>	Spearman r	-0.2955	1	0.165	0.2195	0.414	-0.417	-0.1433
	P (two-tailed)	0.1711		0.4518	0.3142	0.0495	0.0478	0.5143
	P value summary	ns		ns	ns	*	*	ns
<b>Glycogen specific activity</b>	Spearman r	-0.005929	0.165	1	0.6507	0.6897	0.01087	0.3646
	P (two-tailed)	0.9786	0.4518		0.0008	0.0003	0.9607	0.0872
	P value summary	ns	ns		***	***	ns	ns
<b>C3-P specific activity</b>	Spearman r	0.2141	0.2195	0.6507	1	0.9177	0.1637	0.3051
	P (two-tailed)	0.3266	0.3142	0.0008		< 0.0001	0.4556	0.1569
	P value summary	ns	ns	***		****	ns	ns
<b>C6-P specific activity</b>	Spearman r	0.09289	0.414	0.6897	0.9177	1	0.03656	0.1789
	P (two-tailed)	0.6734	0.0495	0.0003	< 0.0001		0.8685	0.4142
	P value summary	ns	*	***	****		ns	ns
<b>Malin binding (<math>\beta</math>-gal activity)</b>	Spearman r	0.6087	-0.417	0.01087	0.1637	0.03656	1	0.6462
	P (two-tailed)	0.0021	0.0478	0.9607	0.4556	0.8685		0.0009
	P value summary	**	*	ns	ns	ns		***
<b>PTG binding (<math>\beta</math>-gal activity)</b>	Spearman r	0.499	-0.1433	0.3646	0.3051	0.1789	0.6462	1
	P (two-tailed)	0.0154	0.5143	0.0872	0.1569	0.4142	0.0009	
	P value summary	*	ns	ns	ns	ns	***	

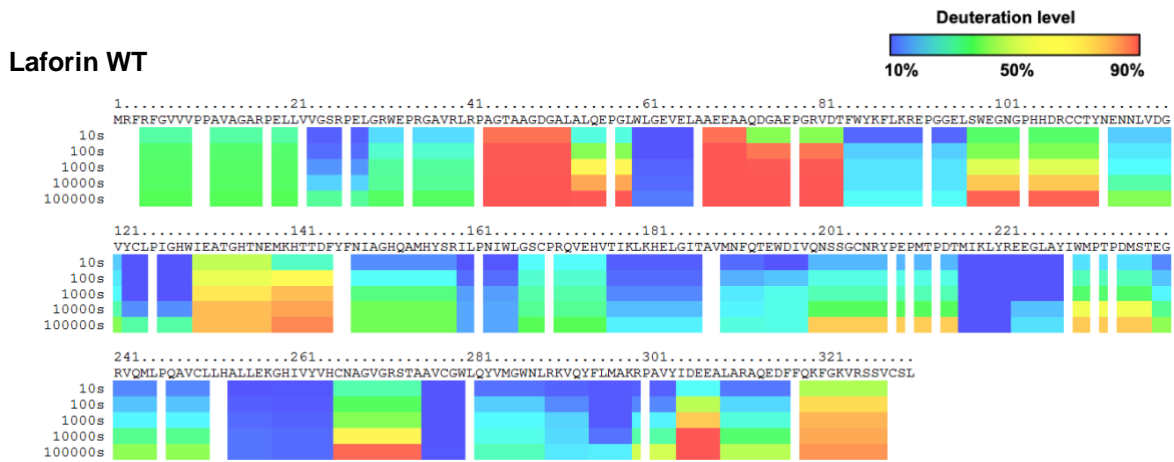
**Table S1. Statistical results from pairwise analysis of properties of laforin mutants, related to Figures 5 and S3.** Analyses were performed using nonparametric Spearman correlations in Prism Graphpad software Spearman correlation coefficients (r), p-values, and p-value summaries are shown (\*  $p \leq 0.05$ , \*\*  $p \leq 0.01$ , \*\*\*  $p \leq 0.001$ , \*\*\*\*  $p \leq 0.0001$ ).

## **Supplemental Data**

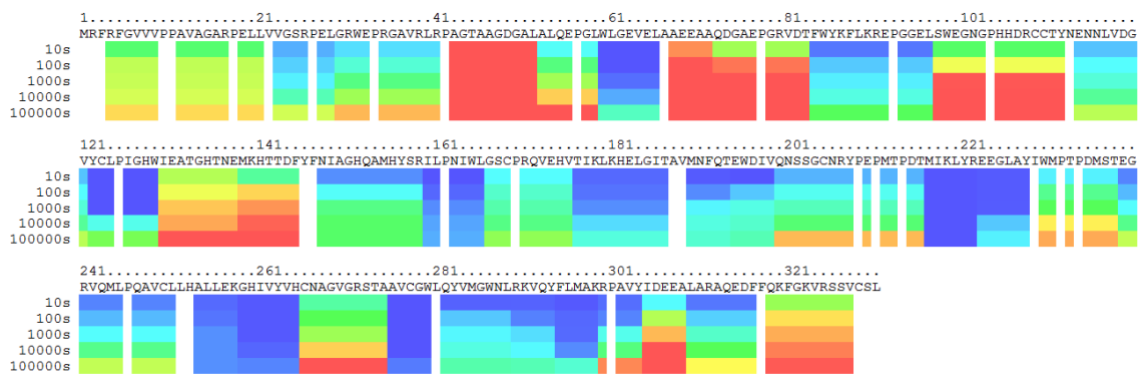
**Data S1. Ribbon maps of HDX results, related to Figure 4.** Deuteration level for WT laforin and LD mutants.

**Data S2. Difference maps of HDX results, related to Figure 4.** Change in deuteration in LD mutants compared to WT laforin. Blue indicates regions with reduced exchange in mutant, red indicates increased exchange in mutant.

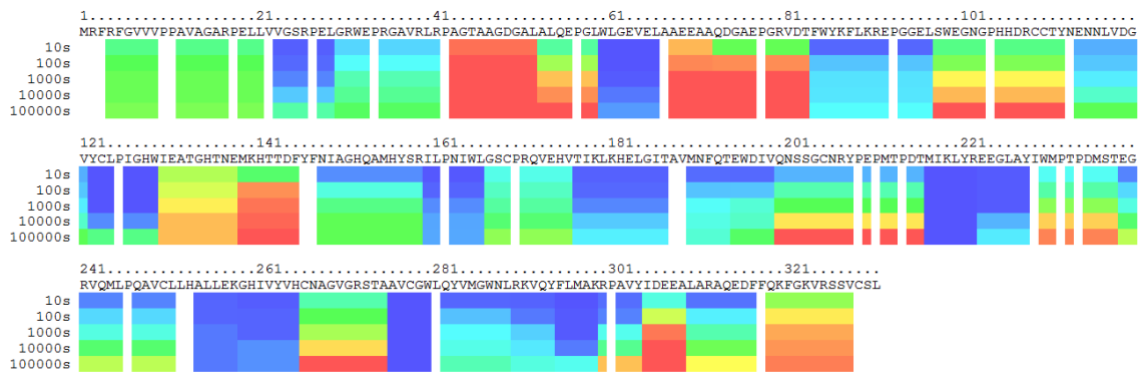
# Data S1



## Laforin R91P

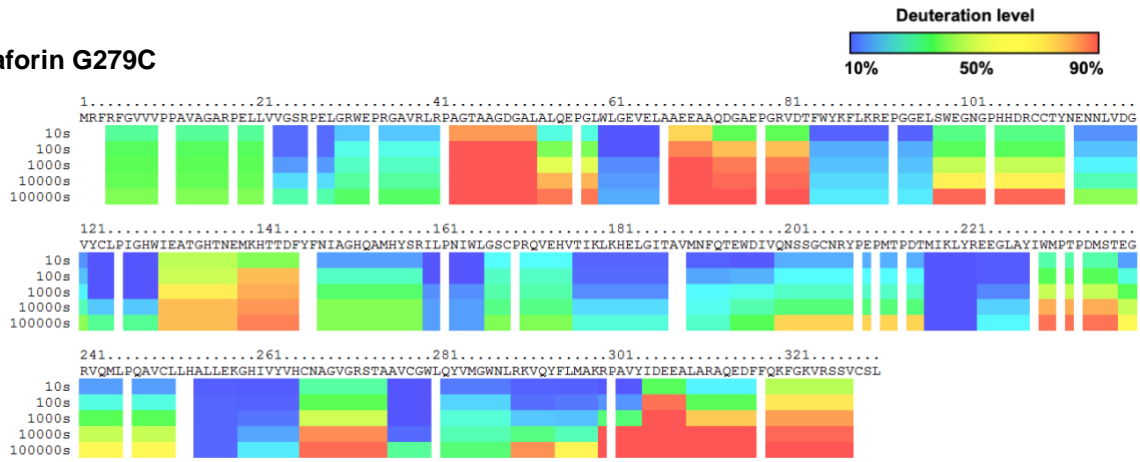


## Laforin P211L

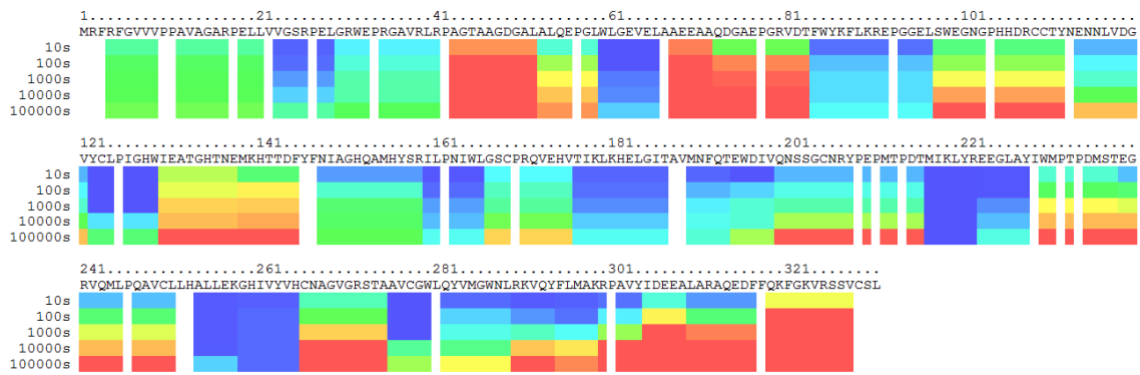


# Data S1

## Laforin G279C

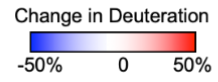


## Laforin F321C





# Data S2



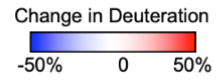
## Laforin R91P



## Laforin P211L



# Data S2



## Laforin G279C



## Laforin F321C

